

## Aging of poly(lactide)/poly(ethylene glycol) blends. Part 2. Poly(lactide) with high stereoregularity

Y. Hu<sup>a</sup>, Y.S. Hu<sup>a</sup>, V. Topolkaraev<sup>b</sup>, A. Hiltner<sup>a,\*</sup>, E. Baer<sup>a</sup>

<sup>a</sup>Department of Macromolecular Science and Center for Applied Polymer Research, Case Western Reserve University Cleveland, OH 44106-7202, USA

<sup>b</sup>Kimberly-Clark Corporation, Neenah, WI 54956, USA

Received 18 March 2003; received in revised form 24 June 2003; accepted 30 June 2003

---

### Abstract

Blending poly(ethylene glycol) (PEG) with poly(lactide) (PLA) decreases the  $T_g$  and improves the mechanical properties. The blends have lower modulus and increased fracture strain compared to PLA. However, the blends become increasingly rigid over time at ambient conditions. Previously, it was demonstrated that a PLA of lower stereoregularity was miscible with up to 30 wt% PEG. Aging was due to slow crystallization of PEG from the homogeneous amorphous blend. Crystallization of PEG depleted the amorphous phase of PEG and gradually increased the  $T_g$  until aging essentially ceased when  $T_g$  of the amorphous phase reached the aging temperature. In the present study, this aging mechanism was tested with a crystallizable PLA of higher stereoregularity. Changes in thermal transitions, solid state structure, and mechanical properties were examined over time. Blends with up to 20 wt% PEG were miscible. Blends with 30 wt% PEG could be quenched from the melt to the homogenous amorphous glass. However, this composition phase separated at ambient temperature with little or no crystallization. Changes in mechanical properties during phase separation reflected increasing rigidity of the continuous PLA-rich phase as it became richer in PLA. Construction of a phase diagram for blends of higher stereoregular PLA with PEG was attempted.

© 2003 Elsevier Ltd. All rights reserved.

**Keywords:** Poly(lactide); Poly(lactide)/poly(ethylene glycol) blends; Aging

---

### 1. Introduction

Poly(lactide) (PLA) is attracting increased attention for applications that require a biodegradable plastic because in a suitable disposal site it will degrade to natural products [1–5]. It also has good physical properties such as high strength, thermoplasticity, and fabricability. However, low deformation at break and high modulus have limited applications of PLA in the packaging industry. Attempts to improve the mechanical properties have focused on biocompatible plasticizers [6–8]. Poly(ethylene glycol) (PEG), the conventional name for low molecular weight (<20,000) poly(ethylene oxide) (PEO), improves elongation at break and softness of PLA [7–11]. At ambient temperature, the desired mechanical properties are achieved by blending PLA with 30 wt% PEG. However, there is evidence that the blend is not stable and the attractive mechanical properties are lost over time [11].

Lactic acid exists as two enantiomeric forms, the D(+) configuration and the naturally occurring L(–) configuration. These produce the corresponding enantiomeric polymers by conservation of the chiral center. Generally, commercial PLA grades are copolymers of L-lactide and D-lactide. The optical purity, defined as  $|L\% - D\%|$ , strongly affects the properties. Optically pure PLA is isotactic and highly crystalline. Decreasing the optical purity reduces the degree of stereoregularity and crystallinity. Poly(L-lactide) with more than 15 mol% D-lactide is amorphous [12].

Many studies indicate that tacticity of a constituent influences miscibility of polymer blends. Most studies focus on blends of poly(methyl methacrylate) (PMMA) because of its availability in both syndiotactic and isotactic forms. In blends with PEO and PEG the composition range of miscibility is larger for syndiotactic PMMA and for atactic PMMA (which contains long syndiotactic sequences) than for isotactic PMMA [13,14]. Similarly, syndiotactic and atactic PMMA are miscible with poly(vinyl chloride) (PVC) over a larger composition range than is isotactic PMMA [15,

---

\* Corresponding author. Tel.: +1-216-368-4186; fax: +1-216-368-6329.  
E-mail address: [pah6@po.cwru.edu](mailto:pah6@po.cwru.edu) (A. Hiltner).

[16]. It is suggested that these differences arise from the free-volume contribution to the energy of mixing.

Stereoregularity of PLA may similarly affect miscibility with PEG and other plasticizers. The phase condition has important implications for aging. However, previous investigations have not addressed this possibility. Blends of low stereoregular PLA with up to 30 wt% PEG are miscible at ambient temperature. Changes in mechanical properties over time are due to slow crystallization of PEG from the homogeneous blend. Depletion of PEG increases the glass transition temperature ( $T_g$ ) of the amorphous phase until aging essentially ceases when  $T_g$  reaches the aging temperature [11]. The present study addresses the effect of stereoregularity on miscibility and aging of PLA/PEG blends. Results obtained with blends of a high stereoregular PLA are compared with findings in the previous study of low stereoregular PLA.

## 2. Experimental

### 2.1. Materials

The study utilized two poly(lactic acid) resins, one with higher stereoregularity (PLA1) and one with lower stereoregularity (PLA2). The specific optical rotation,  $[\alpha]_D^{25}$ , of PLA1 was  $-141$  as measured in chloroform at a concentration of  $1 \text{ g dl}^{-1}$  and  $25^\circ\text{C}$  (Autopol III Polarimeter). From  $[\alpha]_D^{25}$ , the PLA was determined to have a D-lactide content of 5% by assuming  $[\alpha]_D^{25}$  of poly(L-lactic acid) and poly(D-lactic acid) to be  $-156$  and  $156$ , respectively [12]. After annealing at  $100^\circ\text{C}$  for 1000 min, PLA1 exhibited 40% crystallinity with melting temperature of  $151^\circ\text{C}$ , which was consistent with this level of stereoregularity [12]. The PLA1 resin had  $M_w = 190 \text{ kDa}$  and  $M_w/M_n = 1.5$  as determined by gel permeation chromatography (Perkin Elmer Series 200 GPC) using tetrahydrofuran with concentration of  $0.6 \text{ g dl}^{-1}$  at  $40^\circ\text{C}$  and calibration to polystyrene standards. The lower stereoregular PLA2 was described previously [11]. It had D-lactide content of 13%,  $M_w = 160 \text{ kDa}$  and  $M_w/M_n = 1.6$ . It exhibited 2% crystallinity after annealing at  $100^\circ\text{C}$  for 1000 min with melting temperature  $132^\circ\text{C}$ . The poly(ethylene glycol) (PEG) was also described previously [11]. It had molecular weight of 8000 and was highly crystalline, even after quenching the crystallinity was about 95% with melting temperature of  $63^\circ\text{C}$ .

### 2.2. Methods

The polymers were vacuum dried overnight at  $50^\circ\text{C}$  before processing. Melt-blends with compositions PLA1/PEG 90/10, 80/20 and 70/30 wt/wt were prepared using a counter-rotating twin screw extruder operating at  $190^\circ\text{C}$ . To mold the blends into films 0.5 mm thick the pellets were sandwiched between Mylar® sheets and heated at  $185^\circ\text{C}$  for

2 min with minimal pressure, for 2 min at 10 MPa pressure, for six pressure cycles between 10 to 0 MPa to remove air bubbles, for 2 min at 20 MPa, and quenched into ice water. Blend films were stored under ambient conditions ( $23^\circ\text{C}$ , about 50% relative humidity (RH)) or at  $30^\circ\text{C}$  to study the effects of aging.

Uniaxial stress–strain measurements were performed using an Instron model 1123 universal testing machine. Specimens were cut from the films according to ASTM 1708 micro-tensile specifications. The grip separation was 22.3 mm and the specimen width was 4.8 mm. Tests were carried out at a strain rate of  $50\% \text{ min}^{-1}$ . At least two specimens were tested for each condition. Engineering strain was calculated from the crosshead displacement. Engineering stress was defined conventionally as the force per initial unit cross-sectional area.

Differential scanning calorimetry (DSC) was carried out with a Perkin Elmer DSC-7. To obtain the thermal behavior of unaged materials, specimens weighing 5–10 mg were held at  $185^\circ\text{C}$  for 4 min in the DSC, quenched to  $-50^\circ\text{C}$  at  $100^\circ\text{C min}^{-1}$ , and heated to  $185^\circ\text{C}$  at  $10^\circ\text{C min}^{-1}$ . For the aging study, specimens were cut from molded films that had aged for various periods of time and thermograms were obtained with a heating rate of  $10^\circ\text{C min}^{-1}$ . Percent crystallinity was calculated from the melting or crystallization enthalpy using heats of fusion of  $197 \text{ J g}^{-1}$  for PEG [17] and  $94 \text{ J g}^{-1}$  for PLA [12]. The reported crystallinities are normalized to the weight fraction of the constituents in the blend.

Dynamic mechanical thermal analysis (DMTA) was performed on molded films with a DMTA MkII unit from Polymer Laboratories operating in the tensile mode. The relaxation spectrum was scanned from  $-60$  to  $100^\circ\text{C}$  with a frequency of 1 Hz and a heating rate of  $3^\circ\text{C min}^{-1}$ .

Films were microtomed through the thickness at ambient temperature (Ultramicrotome MT6000-XL, RMC, Tucson, AZ) and atomic force microscopy (AFM) was performed on the microtomed surface with a Nanoscope IIIa with MultiMode head and J-scanner. The tapping mode was used at ambient temperature, which was  $30^\circ\text{C}$  in the instrument. Commercial Si probes were chosen with a resonance frequency in the 300 kHz range. Height and phase images were recorded simultaneously.

## 3. Results and discussion

### 3.1. Unaged PLA/PEG blends

Thermograms of quenched PLA1 and PLA1/PEG blends are shown in Fig. 1. Without PEG, PLA1 was amorphous after quenching with  $T_g$  of about  $60^\circ\text{C}$ . Quenched PLA1 did not cold-crystallize upon heating. Quenched PLA1/PEG blends were also amorphous and exhibited a single glass transition in thermograms. Increasing PEG content of the blend caused the  $T_g$  to decrease through ambient

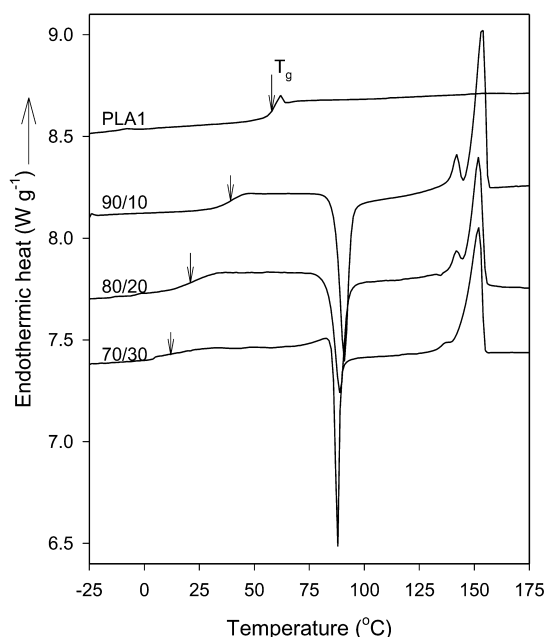


Fig. 1. Thermograms of quenched PLA1 and PLA1/PEG blends with a heating rate of  $10\text{ }^{\circ}\text{C min}^{-1}$ .

temperature to  $12\text{ }^{\circ}\text{C}$  for the blend with 30 wt% PEG. Upon heating the blends at  $10\text{ }^{\circ}\text{C min}^{-1}$  the PEG did not crystallize, however, the PLA1 cold-crystallized at about  $85\text{ }^{\circ}\text{C}$ . Correspondence in the enthalpies of cold-crystallization and subsequent melting confirmed that the quenched blend was amorphous. Cold-crystallization shifted to a slightly lower temperature as the PEG content increased in parallel with the shift in  $T_g$ . The melting temperature of PLA1 was essentially unaffected by blend composition, and the PLA1 crystallinity relative to total PLA1 was constant at about 45%. Double melting peaks in PLA blends have been attributed to lamellar reorganization [7,10].

The dynamic mechanical relaxation behavior of the quenched blends is presented by the temperature dependence of loss tangent ( $\tan \delta$ ), storage modulus ( $E'$ ), and loss modulus ( $E''$ ) in Fig. 2. As in the DSC thermograms, a single glass transition was observed which gradually shifted through ambient temperature as PEG concentration increased. Except for the 70/30 blend the peak temperature in  $\tan \delta$  was always about  $10\text{ }^{\circ}\text{C}$  higher than the  $T_g$  measured from DSC, whereas the peak temperature in  $E''$  correlated closely with  $T_g$  from

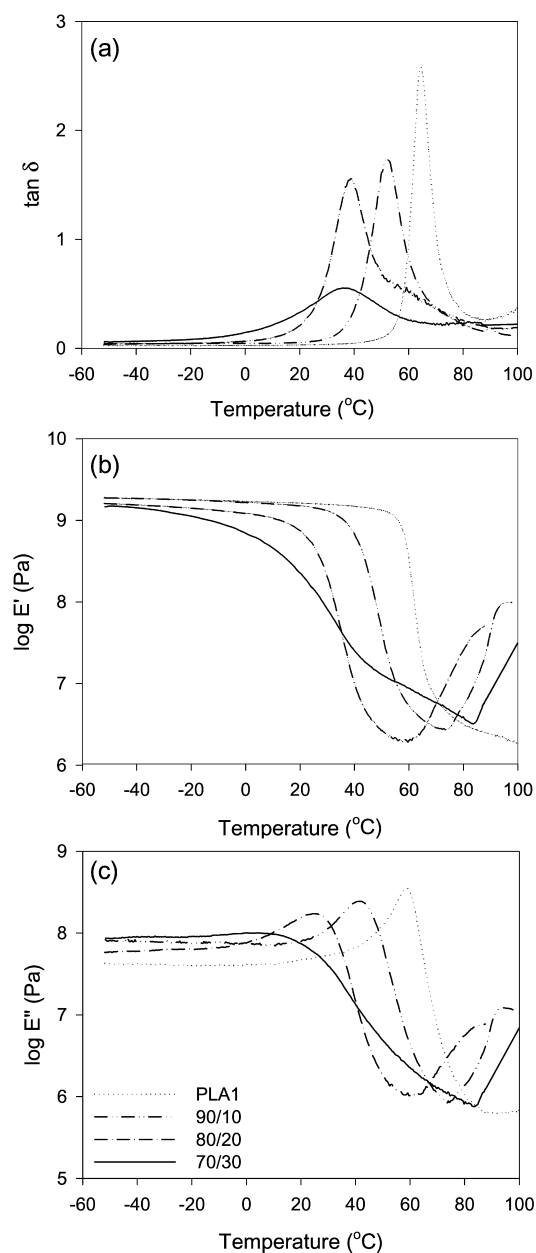


Fig. 2. Dynamic mechanical relaxation behavior of PLA1 and PLA1/PEG blends: (a)  $\tan \delta$ ; (b)  $E'$ ; and (c)  $E''$ .

DSC, Table 1. A large drop in  $E'$  accompanied the  $T_g$ . The increase in  $E'$  and  $E''$  at higher temperatures reflected the onset of PLA1 cold-crystallization.

Compared to DMTA curves of PLA1, 90/10 and 80/20 blends, the glass transition peak in  $\tan \delta$  was noticeably

Table 1  
Effect of PEG content on the thermal and mechanical properties of quenched PLA1/PEG blends

Composition PLA1/PEG	$T_g$ from DSC ( $^{\circ}\text{C}$ )	$T_g$ from $E''$ ( $^{\circ}\text{C}$ )	2% secant modulus (MPa)	Yield stress (MPa)	Fracture strain (%)
100/0	60	59	$2500 \pm 200$	$68 \pm 2$	$3 \pm 0.5$
90/10	39	40	$900 \pm 50$	$26 \pm 1$	$180 \pm 10$
80/20	21	24	$150 \pm 20$	$4 \pm 0.5$	$260 \pm 20$
70/30	12	—	$20 \pm 2$	—	$300 \pm 30$

broader and less intense for 70/30 blends, and the peak temperature was higher than expected based on the DSC results. A gradual decrease in  $E'$  rather than a sharp drop accompanied  $T_g$  and a broad plateau rather than a sharp peak appeared in  $E''$ . The possibility could not be eliminated that this composition underwent some amount of aging at ambient temperature in the 30 min required for preparation and mounting of the DMTA specimen.

The  $T_g$  values from DSC and  $E''$  (with the exception of  $T_g$  from  $E''$  for the 70/30 blend) are plotted in Fig. 3 according to the Fox equation [18]

$$\frac{1}{T_g} = \frac{w_1}{T_{g1}} + \frac{w_2}{T_{g2}} \quad (1)$$

where  $w$  is the weight fraction and the subscripts 1 and 2 refer to the blend constituents. Results from a previous study of PEG blended with PLA2 are included [11]. The  $T_g$  of quenched PLA/PEG blends followed the empirical Fox equation with  $T_g$  for PEG of  $-66^\circ\text{C}$ . It was inferred that the blends formed a single amorphous phase in the melt, and that the phase condition in the melt was preserved when the blends were quenched.

The stress–strain behavior of quenched PLA1/PEG blends was examined at ambient temperature, as shown in Fig. 4. Unmodified PLA1 was a stiff, brittle polymer. It yielded with formation of an unstable neck that fractured almost immediately. The yield stress was approximately 68 MPa and the fracture strain was 4%. Addition of 10% PEG improved the ductility dramatically, Table 1. The yield stress dropped to about 26 MPa and the fracture strain increased to about 200%. Blending with PEG significantly improved the softness of PLA1 and the elongation at break by decreasing the  $T_g$ . The 70/30 blend had  $T_g$  below ambient temperature; it had modulus two orders of magnitude lower than PLA1 and elongation at break of 300%. The 80/20

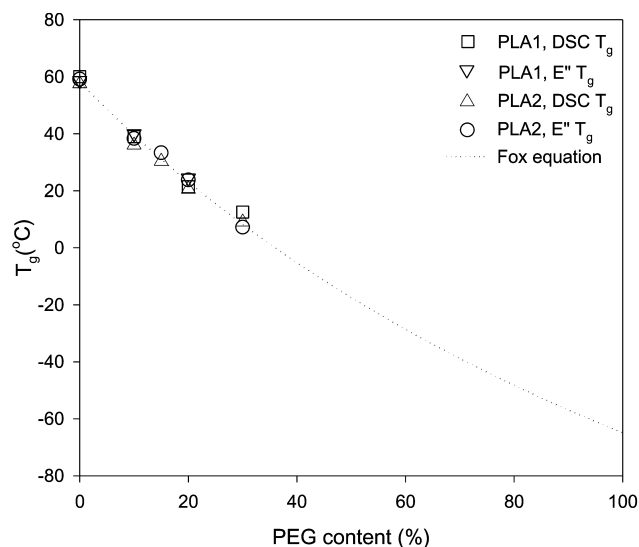


Fig. 3. Dependence of the glass transition temperature from the DSC thermogram and  $E''$  on blend composition. Data for blends of PEG with lower stereoregular PLA2 are taken from Ref. [11].

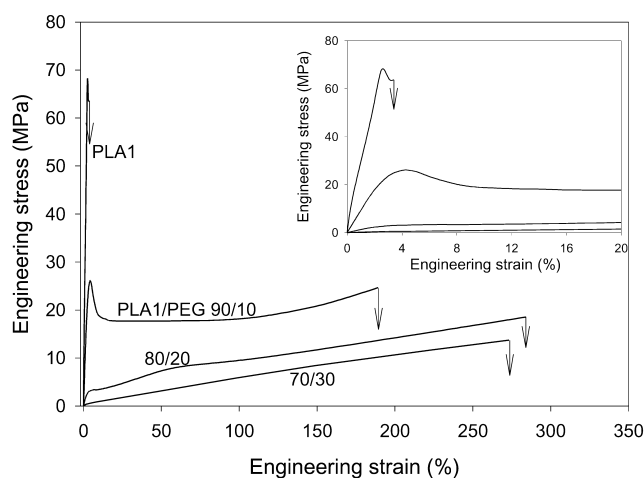


Fig. 4. Tensile stress–strain behavior of quenched PLA1 and PLA1/PEG blends at ambient temperature. The insert shows the modulus and yielding regions on an expanded strain scale.

blend had  $T_g$  coincident with ambient temperature; it exhibited diffuse necking and complex yielding behavior.

### 3.2. Aging of PLA/PEG 70/30 blends

Aging PLA1/PEG 70/30 films under ambient conditions ( $23^\circ\text{C}$ , about 50% RH) produced the changes in tensile properties seen in Fig. 5. With time, the films changed from low modulus elastomer-like materials to higher modulus thermoplastic-like materials. After aging for 720 h the modulus increased by an order of magnitude and the fracture strain decreased from 300 to 160%, Table 2. After 720 h the aging process slowed so that there was very little change in tensile properties between 720 and 3000 h.

Thermograms of aged PLA1/PEG 70/30 are shown in Fig. 6. PEG, by itself, was highly crystallizable. Quenched PEG was about 95% crystalline with a melting temperature of  $63^\circ\text{C}$ . However, PEG in the blends with PLA1 did not crystallize when the blend was quenched from the melt.

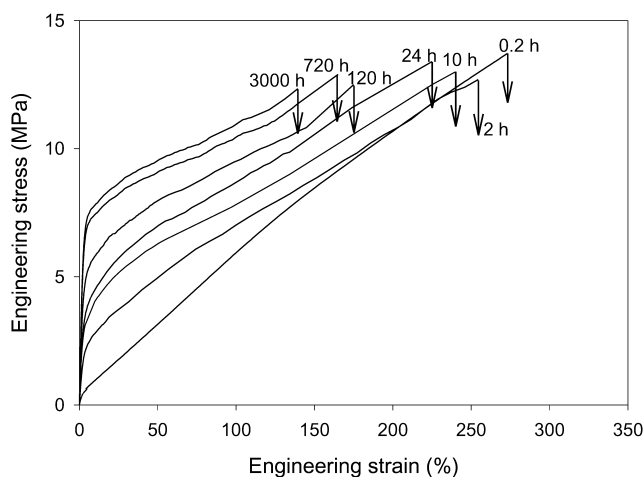


Fig. 5. Effect of aging under ambient conditions ( $23^\circ\text{C}$ , about 50% RH) on the tensile stress–strain behavior of PLA1/PEG 70/30 blends.

Table 2  
Effect of ambient aging on the mechanical properties of quenched PLA1/PEG 70/30 blend

Aging time (h)	2% secant modulus (MPa)	Yield stress (MPa)	Fracture strain (%)
0.2	20 ± 2	–	300 ± 30
2	80 ± 5	2.2 ± 0.3	250 ± 20
10	140 ± 10	3.8 ± 0.3	230 ± 20
24	150 ± 10	4.5 ± 0.3	220 ± 10
120	170 ± 15	5.0 ± 0.2	170 ± 20
720	240 ± 10	7.0 ± 0.3	160 ± 10
3000	250 ± 10	7.5 ± 0.3	150 ± 15

Upon aging, a small melting peak of PEG crystals appeared at 50–60 °C. As the aging time increased, the endotherm grew somewhat larger, however, even after 3300 h the PEG crystallinity was only about 9% as determined from the melting enthalpy. Minimal changes in the cold-crystallization and melting peaks of PLA1 indicated that little if any PLA1 crystallized during aging. Cross-sections of aged 70/30 films exhibited only weak birefringence in the polarized light microscope.

The previous study of PEG blended with low stereoregular PLA2 demonstrated that slow crystallization of PEG from the homogeneous amorphous blend was responsible for aging phenomena including changes in the stress–strain curve [11]. This is illustrated by the parallel time-dependencies of PEG crystallinity and 2% secant modulus of the 70/30 blends, Fig. 7a. The level of PEG crystallinity in these aged blends (70%) approached the high level of crystallinity in PEG alone (95%). In contrast, even though high stereoregular PLA1 and PEG alone readily crystallized to high levels of crystallinity, changes in the stress–strain curve of 70/30 blends could not be attributed to crystallization of one or both

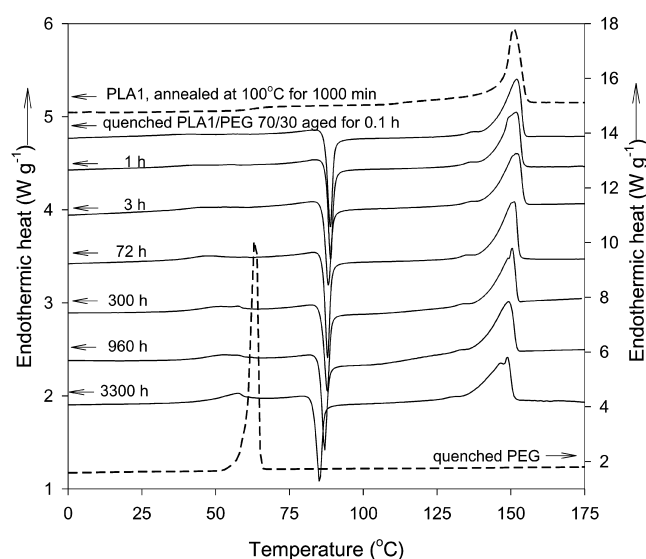


Fig. 6. Effect of aging under ambient conditions (23 °C, about 50% RH) on the thermogram of PLA1/PEG 70/30 blends.

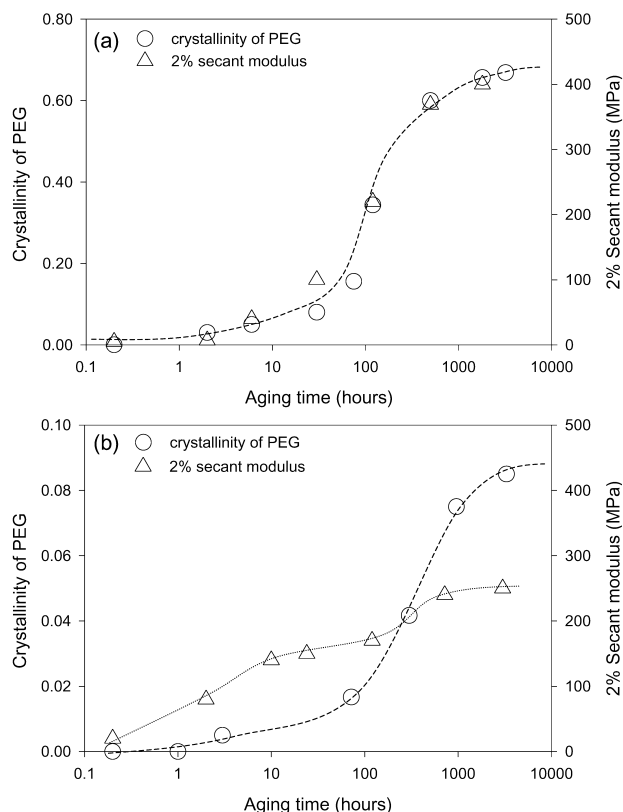


Fig. 7. Change in PEG crystallinity and 2% secant modulus of the PLA/PEG 70/30 blend with aging time: (a) blends of lower stereoregular PLA2, data taken from Ref. [11]; and (b) blends of higher stereoregular PLA1.

constituents. This was evident from the time-dependencies of PEG crystallinity and 2% secant modulus in Fig. 7b. Most of the modulus increase occurred in the first 10 h of aging, whereas the largest increase in PEG crystallinity occurred after 100 h. Moreover, even after aging for 3300 h the PEG crystallinity reached a level of only about 9% in the PLA1 blend. Clearly, physical changes other than crystallization were responsible for aging of PLA1 blends.

The morphology of the aged 70/30 blends was probed by AFM. Because the temperature in the AFM was slightly higher than ambient temperature, aging was performed at 30 °C in order to obtain stable morphologies for examination in this very sensitive instrument. Thermograms of the 70/30 blend aged at 30 °C were equivalent to those in Fig. 6, thereby confirming that the small increase in aging temperature from 23 to 30 °C did not alter the aging process except perhaps to accelerate it slightly. The phase image in Fig. 8 from the interior of a film that was aged for 48 h shows phase separation with domains about 0.1 to 0.3 μm in diameter dispersed in a continuous matrix. The higher modulus matrix material appears brighter in the phase image and the softer dispersed phase appears darker. Based on relative hardness of the phases, the dispersed phase is identified as being PEG-rich with lower  $T_g$ , the matrix is



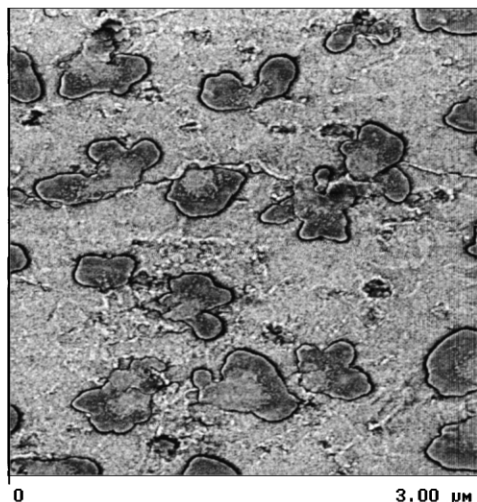


Fig. 8. AFM phase image of the PLA1/PEG 70/30 blend after aging at 30 °C for 40 h.

PLA-rich with higher  $T_g$ . The irregular shape of the dispersed phase domains contrasts to the typical spherical shape encountered in blends that phase-separate in the melt. The unusual shape is attributed to retarded droplet coalescence caused by the increasing viscosity of the matrix as it becomes richer in PLA1 and the  $T_g$  approaches the aging temperature. The absence of a regular crystalline texture in either phase suggests that both are essentially amorphous.

Evidence for two glass transitions was sought in dynamic mechanical relaxation measurements of the aged 70/30 blends. Before aging, the temperature of the  $\tan \delta$  peak of the quenched film was much higher than expected based on DSC results. Phase separation could have started in the 30 min required for preparation and mounting of the DMTA specimen. After 2 h, the peak in  $\tan \delta$  and the corresponding drop in  $E'$  shifted to higher temperature, Fig. 9. After the blend aged for 120 h, melting of PEG crystals obscured the glass transition peak in the  $\tan \delta$  curve, however the broad peak in  $E''$  at about 20 °C was identified with the glass transition of the PLA-rich continuous phase. A new peak at low temperature was discernable in the  $\tan \delta$  curve of the aged blend. Appearance of the low temperature peak was very clear in the  $E''$  curve of the blend after aging for 2 h. The peak in  $E''$  at about –35 °C was assigned to the glass transition of the PEG-rich dispersed phase.

### 3.3. Aging of PLA/PEG 80/20 and 90/10 blends

Aging of the 80/20 blend produced the thermograms in Fig. 10. After 48 h a small endothermic peak at about 55 °C corresponded to melting of PEG crystals. The PEG crystallinity was about 12%. The PLA1 remained essentially amorphous as indicated by the prominent cold-crystallization and melting peaks.

The  $\tan \delta$  and  $E''$  curves of the 80/20 blend showed a single peak that decreased in intensity and shifted to higher

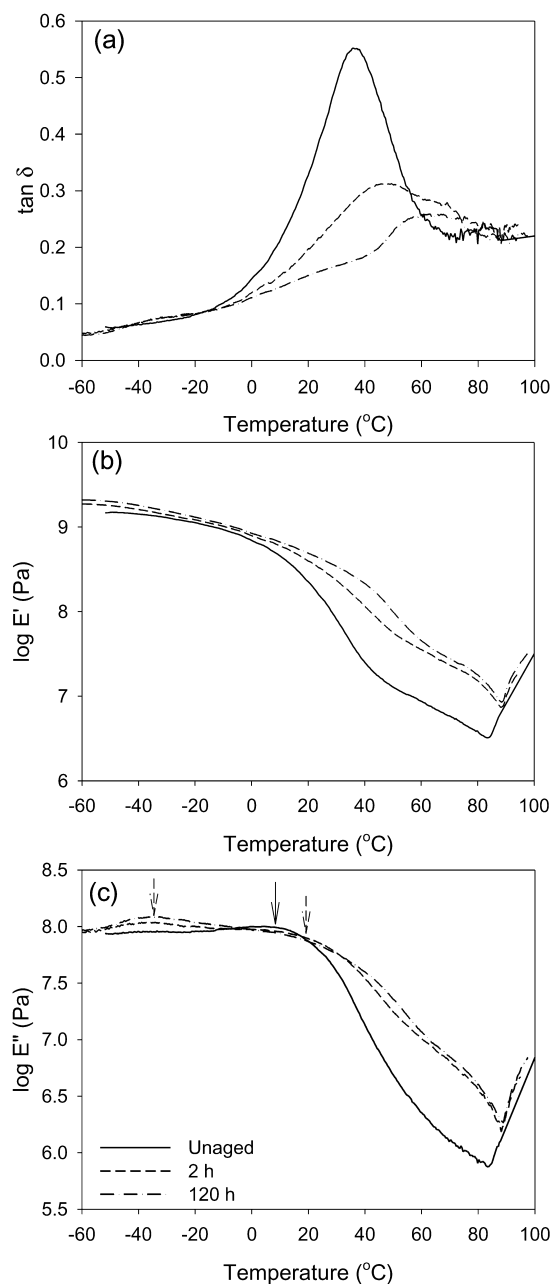


Fig. 9. Effect of aging at 30 °C on the dynamic mechanical relaxation behavior of PLA1/PEG 70/30: (a)  $\tan \delta$ ; (b)  $E'$ ; and (c)  $E''$ .

temperature as the blend aged. The peak in  $E''$  shifted from 23 to 27 °C after aging for 720 h, Fig. 11. There was no evidence of a low temperature peak in  $E''$ . This composition appeared to be miscible at the aging temperature.

An AFM phase image of the 80/20 blend that was aged for 48 h showed no evidence of phase separation, Fig. 12. Aging of this composition appeared to follow the process of PEG crystallization from the homogeneous amorphous blend. The granular texture with no evidence of ordered crystalline structures was consistent with the low PEG crystallinity of this specimen, about 12%.

The 90/10 blend exhibited essentially no changes in the

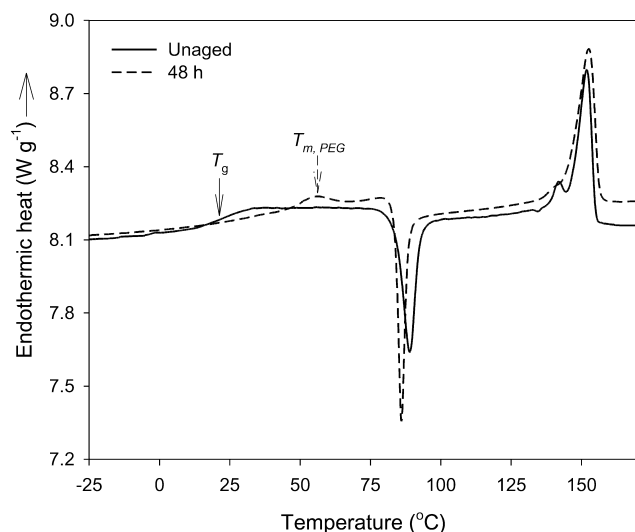


Fig. 10. Effect of aging at 30 °C on the thermogram of PLA1/PEG 80/20.

DMTA curves after aging for 200 h at 30 °C, Fig. 13. With  $T_g$  above ambient temperature at 38 °C from  $E''$ , this composition was in the glassy state at the aging temperature.

### 3.4. Model for aging of PLA/PEG blends

The higher stereoregular PLA1 used in this study was crystallizable. However, PLA1 did not crystallize readily as indicated by the absence of cold crystallization and melting peaks in thermograms of quenched PLA1. Blending with PEG accelerated crystallization to the extent that PLA1 in quenched blends underwent cold crystallization during heating. However, PLA1 crystallization remained slow enough that blends with up to 30 wt% PEG were readily quenched to the amorphous state. Furthermore, the PLA1 constituent did not crystallize to a noticeable extent during aging under ambient conditions as indicated by the continued presence of a prominent cold-crystallization peak in DSC thermograms. With the PLA1 constituent in the amorphous state it was possible to extract the effects of stereoregularity by directly comparing blends of PLA1 with blends of PLA2 studied previously [11].

All the results indicated that PEG was miscible with PLA in compositions up to 20% PEG regardless of stereoregularity. In these compositions, blends of PLA1 and PLA2 were essentially indistinguishable in their thermal behavior as determined by DSC and DMTA. Aging of the 80/20 blends was completely consistent with the process described previously for miscible blends [11], in which crystallization of PEG depleted the amorphous regions of that constituent and gradually increased  $T_g$  until aging essentially ceased when  $T_g$  reached the aging temperature. The extent of aging was determined by the compositional dependence of  $T_g$  rather than by the intrinsic crystallizability of the blend constituents. Crystallization to a level of about 12% sufficiently depleted the amorphous phase of PEG to raise

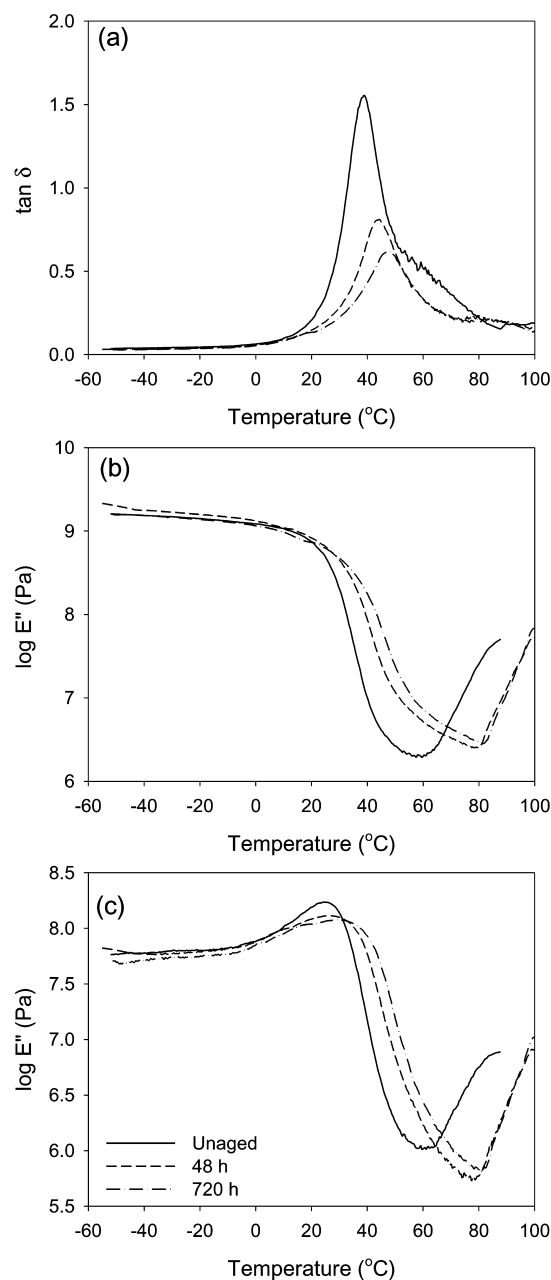


Fig. 11. Effect of aging at 30 °C on the dynamic mechanical relaxation behavior of PLA1/PEG 80/20: (a)  $\tan \delta$ ; (b)  $E'$ ; and (c)  $E''$ .

$T_g$  of the 80/20 blends to ambient temperature. The 90/10 blends with  $T_g$  above ambient temperature did not exhibit aging.

The 70/30 blends of higher and lower stereoregularity behaved differently. The PLA2 formed miscible blends with PEG in the 70/30 composition [11]. In contrast, PLA1 was not completely miscible with PEG in this composition and underwent phase separation at ambient temperature, as indicated by the AFM phase image (Fig. 8) and supported by DMTA (Fig. 9). It is not unusual for tacticity of one constituent to affect miscibility. The isotactic form of PMMA was found to be miscible with PEG over a smaller

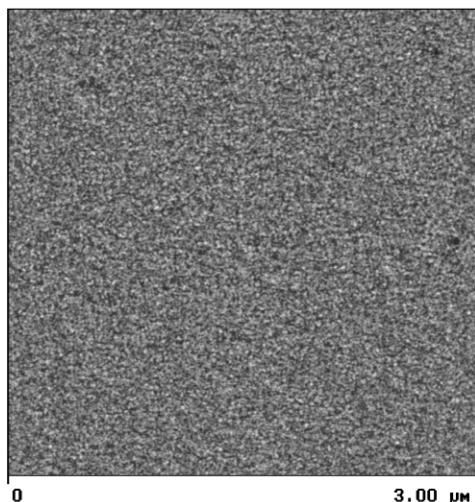


Fig. 12. AFM phase image of the PLA1/PEG 80/20 blend after aging at 30 °C for 48 h.

composition range than were the syndiotactic and atactic forms [13,14]. It seems reasonable that the causes are similar.

Phase separation apparently started at ambient temperature almost immediately after the 70/30 blend of PLA1 was quenched from the melt. This was inferred from inconsistencies in the  $T_g$  behavior. Whereas DSC thermograms obtained immediately after quenching showed  $T_g$  at the temperature expected for a miscible blend according to Eq. (1),  $T_g$  in DMTA curves obtained 0.5 h after quenching was broader and at a higher temperature than expected. This behavior was consistent with onset of phase separation and appearance of a PLA-rich continuous phase. Phase separation was essentially complete within 48 h. This was inferred from the AFM image, which showed clear phase separation, and from the appearance of a low temperature peak in  $E''$ , which corresponded to the  $T_g$  of the PEG-rich phase.

It appeared that phase separation, rather than PEG crystallization, was the primary aging process in 70/30 blends. Most of the changes in stress-strain behavior occurred within 10 h although the amount of PEG crystallinity was insignificant at this time point. As illustrated by the 2% secant modulus (Fig. 7b), changes in mechanical properties reflected increasing rigidity of the continuous PLA-rich phase as it became richer in the PLA constituent. Crystallization of PEG produced some additional aging at longer times, however the amount of PEG crystallinity was only about 9%, compared to 70% in the miscible 70/30 blend of lower stereoregular PLA2, and the change in 2% secant modulus that accompanied crystallization was likewise much smaller.

It was possible to estimate the phase compositions of the 70/30 blends. From the  $T_g$  of  $-35$  °C, Eq. (1) gave the composition of the PEG rich phase as PLA1/PEG 35/65. The softer PEG-rich phase appeared as the minor phase in AFM images and the volume fraction,  $\phi_{\text{PEG}}$ ,

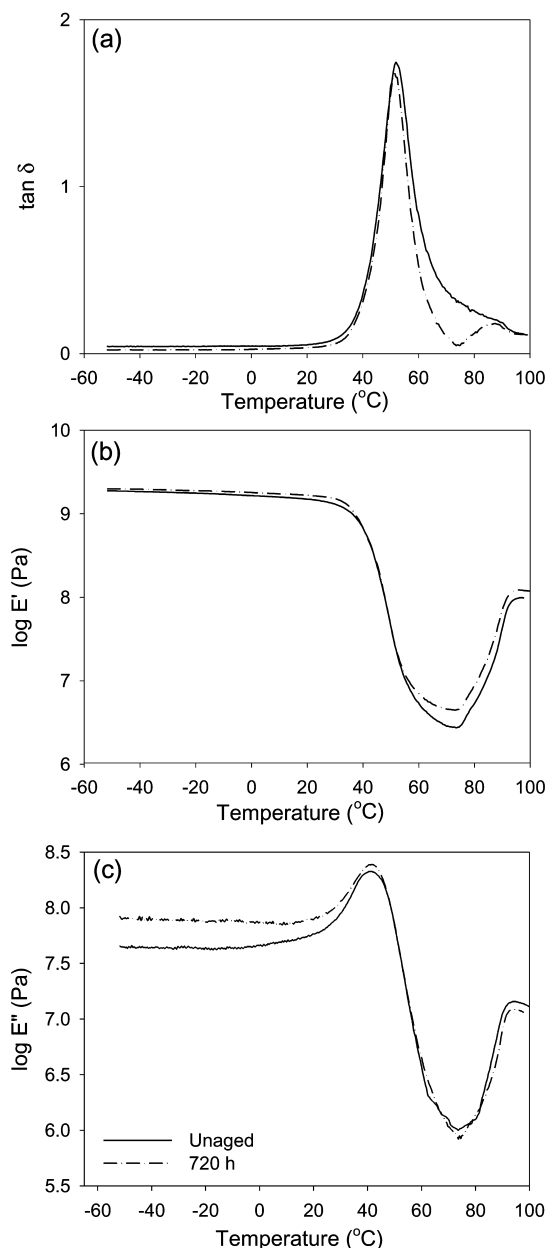


Fig. 13. Effect of ambient aging on the dynamic mechanical relaxation behavior of PLA1/PEG 90/10: (a)  $\tan \delta$ ; (b)  $E'$ ; and (c)  $E''$ .

was determined to be  $0.20 \pm 0.02$  [19,20]. Assuming that weight fraction and volume fraction were equivalent, the weight fraction of each constituent,  $W_{i,\text{PLA}}$  in the PLA-rich phase was calculated as

$$W_{i,\text{PLA}} = \frac{W_i - W_{i,\text{PEG}}\phi_{\text{PEG}}}{1 - \phi_{\text{PEG}}} \quad (2)$$

where  $W_i$  is the weight fraction of the constituent in the unaged blend and  $W_{i,\text{PEG}}$  is the weight fraction of the constituent in the PEG-rich phase of the aged blend. The calculated composition of the PLA-rich phase was PLA1/PEG 79/21. Ambient temperature was slightly above the  $T_g$  of the PLA-rich phase, which was



determined from Eq. (1) to be 20 °C. Possibly the PLA-rich phase aged in the same manner as the miscible 80/20 blends. The low level of PEG crystallinity, 9%, and correspondingly slight increase in 2% secant modulus would be consistent with this speculation.

A phase diagram was constructed for the higher stereoregular PLA1, Fig. 14. All the blends studied could be quenched from the one-phase melt at 185 °C to the amorphous glass. The solid line defined the glass transition of the homogeneous blend. In the glassy state, the blends did not change over time. Thus at 30 °C the 90/10 composition remained in the glassy region. The 80/20 and 70/30 compositions were above the solid line. The 70/30 blends formed two phases whose compositions defined points on the dashed coexistence curve. The 80/20 blends were just outside the 2-phase region and therefore remained homogeneous.

The PLA1/PEG blends are inferred to have an upper critical solution temperature (UCST). However, the dashed line only qualitatively defines the coexistence line. Much of the phase diagram is not readily accessible. Raising the temperature of the 70/30 blends in an effort to approach the UCST results in crystallization of PLA1. Efforts to extend the diagram to lower temperatures with blends of higher PEG content fail because PEG begins to crystallize during quenching if the blend contains 50 wt% or more PEG [9,10]. In this regard, it is interesting that the PEG-rich phase of the 70/30 blends does not crystallize. Possibly the PEG-rich domains are too small to contain nuclei. The crystallization habit of PEG from the melt or from the homogeneous blend is formation of very large spherulites [11,21,22], which is consistent with low nucleation density.

#### 4. Conclusions

The effect of stereoregularity of PLA in blends with PEG was studied. Although some of the blend constituents were crystallizable, the blends could be quenched from the melt

to the homogeneous amorphous glass. Blends with up to 30 wt% PEG exhibited a single  $T_g$  that depended on composition in accordance with the Fox relationship. Addition of 30 wt% PEG put  $T_g$  below ambient temperature and thereby decreased the modulus and increased the ductility of this relatively rigid, brittle thermoplastic. However blends with 30 wt% PEG were not stable at ambient temperature. With time the modulus increased and the elongation at break decreased. The origin of aging in this composition depended on stereoregularity of the PLA. Lower stereoregular PLA2 aged by crystallization of PEG from the homogeneous blend. The increase in modulus that accompanied aging reflected both the increasingly glassy nature of the matrix as it was depleted of PEG and the reinforcing effect of PEG spherulites. The PLA1 of higher stereoregularity was miscible with PEG over a smaller composition range. Over time a blend with 30 wt% PEG underwent phase separation at ambient temperature with formation of essentially amorphous PLA-rich and PEG-rich phases. The modulus of the continuous PLA-rich phase increased as formation of a PEG-rich phase depleted it of PEG. It was inferred that blends of PEG with higher stereoregular PLA1 possessed an upper critical solution temperature.

#### Acknowledgements

The generous financial and technical support of the Kimberly-Clark Corporation is gratefully acknowledged.

#### References

- [1] Dorgan J, Lehermeier J, Palade L, Cicero J. *Macromol Symp* 2001; 175:55.
- [2] Jacobsen S, Degee PH, Fritz HG, Dubois PH, Jerome R. *Polym Engng Sci* 1999;39:1311.
- [3] Grijpma DW, Van Hofslot R, Super H, Nijenhuis A, Pennings AJ. *Polym Engng Sci* 1994;34:1674.
- [4] Sinclair RG. *ANTEC* 1987;87:1214.
- [5] Kricheldorf HR, Kreiser-Saunders I. *Macromol Symp* 1996;103: 85.
- [6] Jacobsen S, Fritz HG. *Polym Engng Sci* 1999;39:1303.
- [7] Martin O, Averous L. *Polymer* 2001;42:6209.
- [8] Ljungberg N, Wesslen B. *J Appl Polym Sci* 2002;86:1227.
- [9] Yang JM, Chen HL, You JW, Hwang JC. *Polym J* 1997;29:657.
- [10] Nijenhuis A, Colstee E, Grijpma DW, Pennings AJ. *Polymer* 1996;37: 5849.
- [11] Hu Y, Rogunova M, Topolkaraev V, Hiltner A, Baer E. *Polymer* 44 (20) doi: 10.1016/S0032-3861(03)00614-1.
- [12] Tsuji H, Ikada Y. *Macromol Chem Phys* 1996;197:3483.
- [13] Silvestre C, Commimo S, Martuscelli E, Karasz FE, MacKnight WJ. *Polymer* 1987;28:1190.
- [14] Hamon L, Grohens Y, Soldera A, Holl Y. *Polymer* 2001;42:9697.
- [15] Schurer JW, de Boer A, Challa G. *Polymer* 1975;16:201.
- [16] Vorenkamp EJ, ten Brinke G, Meijer JG, Jager H, Challa G. *Polymer* 1985;26:1725.
- [17] Campbell C, Viras K, Richardson MJ, Masters AJ, Booth C. *Makromol Chem* 1993;194:799.

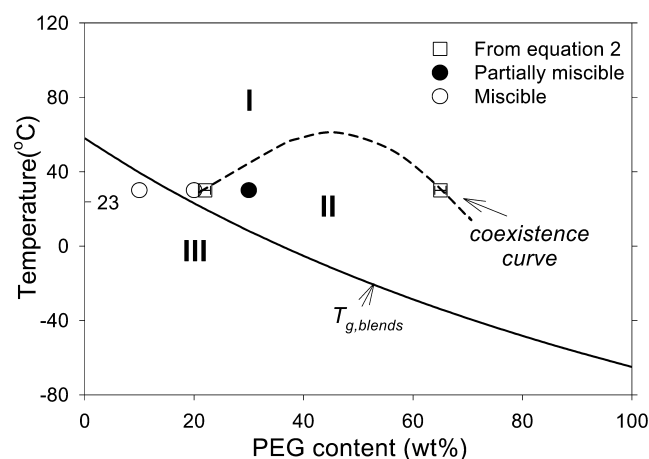


Fig. 14. Schematic showing the phase diagram of PLA1/PEG blends.

- [18] Olabisi O, Mobeson LM, Shaw MT. Polymer–polymer miscibility. New York: Academic Press; 1979.
- [19] Chen HY, Chum SP, Hiltner A, Baer E. *Macromolecules* 2001;34:4033.
- [20] Stephens CH, Hiltner A, Baer E. *Macromolecules* 2003;36:2733.
- [21] Nakafuku C, Sakoda M. *Polym J* 1993;25:909.
- [22] Sheth M, Kumar BA, Dave V, Gross RA, McCarthy SP. *J Appl Polym Sci* 1997;66:1495.